

# Substituent effect on the photoinduced electron-transfer reaction of *para*-substituted triphenylphosphines sensitised by 9,10-dicyanoanthracene

2 PERKIN

Mitsunobu Nakamura,<sup>\*a</sup> Masamichi Miki<sup>a</sup> and Tetsuro Majima<sup>\*b</sup>

<sup>a</sup> Department of Engineering Science, Himeji Institute of Technology, Shosha 2167, Himeji, Hyogo 671-2201, Japan

<sup>b</sup> The Institute of Scientific and Industrial Research, Osaka University, Mihogaoka 8-1, Ibaraki, Osaka 567-0047, Japan

Received (in Cambridge, UK) 28th February 2000, Accepted 17th April 2000

Published on the Web 5th June 2000

The photoinduced electron-transfer reaction of *para*-substituted triphenylphosphines sensitised by 9,10-dicyanoanthracene (DCA) occurred in acetonitrile containing 2 vol% water to form the corresponding triphenylphosphine oxide. Transient absorption spectral measurements were carried out during 355 nm laser flash photolysis of a mixture of the phosphine and DCA. The electron transfer from the phosphine to singlet excited DCA initiated the reaction. A *para* substituent on the benzene ring affects the quantum yields of the phosphine radical cation and phosphine oxide. The back electron transfer from the DCA radical anion to the phosphine radical cation governed the quantum yield of the phosphine radical cation. The quantum yield of the phosphine oxide was dependent on the conjugation between the  $\pi$ -electron of the benzene ring and the  $n$ -electron of the phosphorus atom in the phosphine radical cation. The phosphine oxide forms through nucleophilic attack of H<sub>2</sub>O toward the phosphorus atom of the phosphine radical cation, producing the phosphoranyl radical.

## Introduction

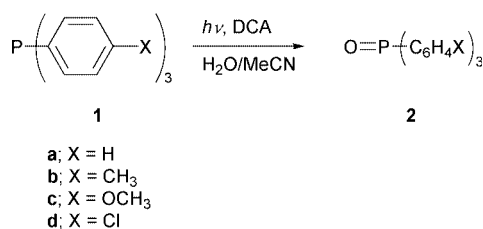
Radical cations of trivalent phosphorus compounds have attracted interest as reaction intermediates in organic reactions, and have been widely investigated from both the mechanistic and the synthetic points of view. Photoinduced electron-transfer reactions sensitised by 1,4-dicyanonaphthalene, 9,10-dicyanoanthracene (DCA), or 9-methylacridinium perchlorate are capable of generating the radical cations of trivalent phosphorus compounds. It is known on the basis of product analyses that the radical cations of phosphines and phosphites react with nucleophiles, such as water and alcohol, to yield phosphine oxides and phosphates.<sup>1</sup> However, we have reported the DCA-sensitised photoinduced electron-transfer reaction of tri-1-naphthyl phosphate, which is a pentavalent phosphorus compound.<sup>2</sup> The radical cation of tri-1-naphthyl phosphate forms the intramolecular dimer radical cation between the two naphthyl groups from which the binaphthyl radical cation eliminates. The O–P(O)–O spacer between the two naphthyl groups is responsible for the elimination of the binaphthyl radical cation; no reaction takes place in the radical cations of 1,3-dinaphthylpropane and bis(1-naphthyl-oxy)methane, which have CH<sub>2</sub>–CH<sub>2</sub>–CH<sub>2</sub> and O–CH<sub>2</sub>–O spacers, respectively. The elimination of the binaphthyl radical cation is characteristic of the radical cation of tri-1-naphthyl phosphate.

Recently we have found that the *para* substitution of triphenylphosphine radical cations affects their reaction efficiency. Electron-donating character present in the *para* substituent shifted the absorption bands of the phosphine radical cations to longer wavelengths and decreased the quantum yield of the phosphine oxide. In this paper, we report on the DCA-sensitised photoinduced electron-transfer reaction of *para*-substituted triphenylphosphine with respect to the reaction efficiency of the phosphine radical cation, on the basis of the spectroscopic measurements and product analyses.

## Results

### Photoreaction of *para*-substituted triphenylphosphine sensitised by DCA

Upon photoirradiation (>355 nm) of a mixture of DCA ( $5.0 \times 10^{-5}$  mol dm<sup>-3</sup>) and triphenylphosphine **1** ( $1.0 \times 10^{-2}$  mol dm<sup>-3</sup>) in acetonitrile containing 2 vol% water under an argon atmosphere, triphenylphosphine oxide **2** was produced (Scheme 1). The quantum yield of **2** decreased with an increase



Scheme 1

in the electron-donating character of the *para* substituent of **1** (Table 1). Similar photoirradiation of a mixture of DCA and **1a** in acetonitrile containing H<sub>2</sub><sup>18</sup>O (H<sub>2</sub><sup>18</sup>O:H<sub>2</sub><sup>16</sup>O = 1:9 atom ratio) was also carried out to clarify the origin of the oxygen atom in **2a**. GC-MS analyses of the irradiated solution showed an M + 2 peak with 11% of the intensity of the peak in **2a**. This value was 6% higher than that of **2a** (5%) formed in the photoirradiation of the mixture of **1a** and DCA in acetonitrile containing H<sub>2</sub>O. It is clear that the increase in the M + 2 peak intensity is a consequence of the formation of **2a**-<sup>18</sup>O using an <sup>18</sup>O-enriched water molecule. Therefore, the oxygen atom of **2** originates from a water molecule. Photoirradiation of a mixture of **1a** and DCA in dry acetonitrile under an argon atmosphere gave a trace amount of **2a** that is probably formed by reaction with the residual water in acetonitrile.

**Table 1** The  $k_q\tau$ ,  $k_q$ ,  $E^{\text{ox}}$ , and  $\Delta G$  values of **1**

	<b>1a</b>	<b>1b</b>	<b>1c</b>	<b>1d</b>
$\phi_2$	0.19	0.10	0.02	0.26
$\phi_{1^+}$	0.44	0.23	0.13	0.50
$\phi_2/\phi_{1^+}$	0.43	0.43	0.15	0.52
$k_q\tau/\text{dm}^3 \text{ mol}^{-1}$	281	268	345	265
$k_q/10^{10} \text{ dm}^3 \text{ mol}^{-1} \text{ s}^{-1}$	1.9	1.8	2.3	1.8
$E^{\text{ox}}/\text{V}$	1.00	0.90	0.78	1.39
$\Delta G_{\text{et}}/\text{kcal mol}^{-1}$	-25.8	-27.8	-30.9	-22.6
$\Delta G_{-\text{et}}/\text{kcal mol}^{-1}$	-51.4	-49.1	-46.3	-60.4
$k_{-\text{et}}/10^9 \text{ s}^{-1}$	0.64	1.7	3.3	0.50

Photoirradiation of a mixture of **1a** and DCA in water–acetonitrile with 2:98 volume ratio containing NaOH was also carried out. The quantum yield of **2a** ( $\phi_{2a}$ ) increased to 0.38–0.43 in the presence of  $1.0 \times 10^{-5}$ – $10^{-3} \text{ mol dm}^{-3}$  NaOH. These  $\phi_{2a}$  values are higher than that in the absence of NaOH. This result suggests that **2a** is formed *via* nucleophilic attack of  $\text{OH}^-$ .

### Fluorescence measurement

Fluorescence of DCA in dry acetonitrile ( $5.0 \times 10^{-5} \text{ mol dm}^{-3}$ ) was quenched by **1** without the formation of a new emission band in the range of 400–700 nm. Stern–Volmer analysis gives the constant,  $k_q\tau$ , where  $k_q$  is rate constant of fluorescence quenching and  $\tau$  is fluorescence lifetime. The  $k_q$  value of the quenching of the singlet excited DCA ( $^1\text{DCA}^*$ ) by **1** is equal to the rate constant ( $k_{\text{et}}$ ) of the electron transfer from **1** to  $^1\text{DCA}^*$  ( $k_q = k_{\text{et}}$ ). The  $k_{\text{et}}$  value can be calculated from the  $k_q\tau_{\text{DCA}}$  value given from the Stern–Volmer analysis and the lifetime of  $^1\text{DCA}^*$  ( $\tau_{\text{DCA}}$ ) measured directly by the single photon counting method. Values of  $k_q\tau = 265$ – $345 \text{ dm}^3 \text{ mol}^{-1}$  were obtained (Table 1). Using  $\tau_{\text{DCA}} = 14.9 \text{ ns}$  in acetonitrile,<sup>3</sup>  $k_q$  values of  $1.8 \times 10^{10}$ – $2.3 \times 10^{10} \text{ dm}^3 \text{ mol}^{-1} \text{ s}^{-1}$  were calculated. These  $k_q$  values are approximately equal to the diffusion-controlled rate constant in acetonitrile at room temperature ( $k_{\text{diff}} = 2.0 \times 10^{10} \text{ dm}^3 \text{ mol}^{-1} \text{ s}^{-1}$ ). Therefore, the  $^1\text{DCA}^*$  quenching by **1** occurs at the diffusion-controlled rate. It has also been reported that **1a** quenches DCA fluorescence in benzene with a rate constant of  $1.1 \times 10^{10} \text{ dm}^3 \text{ mol}^{-1} \text{ s}^{-1}$  (ref. 4). The quenching rate constant in benzene is equal to the diffusion-controlled rate constant in benzene at room temperature ( $k_{\text{diff}} = 1.1 \times 10^{10} \text{ dm}^3 \text{ mol}^{-1} \text{ s}^{-1}$ ).

### Oxidation potential and absorption spectra

Oxidation potentials,  $E^{\text{ox}}$ , of **1a–d** were measured by cyclic voltammetry using a platinum electrode at  $1.0 \times 10^{-2} \text{ mol dm}^{-3}$  in dry acetonitrile containing  $0.10 \text{ mol dm}^{-3} \text{ Bu}_4\text{NClO}_4$  as a supporting electrolyte. Compounds **1a–d** were oxidised in the region 0.78–1.39 V (Table 1). It is known that free energy change is exergonic when an electron transfer occurs at a diffusion-controlled rate. The free energy change during the electron transfer is calculated from the oxidation and reduction potentials of the donor and acceptor molecules, respectively, and the excitation energy according to the Rehm–Weller equation.<sup>5</sup> The half-wave reduction potential of DCA and the excitation energy of  $^1\text{DCA}^*$  have been reported to be  $-0.98 \text{ V}$  (vs. SCE) and  $66.4 \text{ kcal mol}^{-1}$ , respectively. Since we also measured the half-peak oxidation potentials of **1a–d**, the free energy changes in the electron transfer from **1** to  $^1\text{DCA}^*$  ( $\Delta G_{\text{et}}$ ) were calculated to be negative (Table 1). These results indicate that the electron transfer is exergonic. The free energy change of the back electron transfer ( $\Delta G_{-\text{et}}$ ) is also calculated from  $E_{\text{DCA}}^{\text{red}} + E^{\text{ox}}_1$ , which are the reduction potential of DCA and the oxidation potential of **1**, respectively. The negative  $\Delta G_{-\text{et}}$  values in Table 1 indicate that the back electron transfer from  $\text{DCA}^{\cdot-}$  to  $\mathbf{1}^{\cdot+}$  also occurs exergonically. Tordo and co-workers have concluded that the HOMO of triphenylphosphine is the non-bonding orbital (n-orbital) of the phosphorus.<sup>6</sup> Therefore, an electron is removed from the n-orbital of the phosphorus

to give  $\mathbf{1}^{\cdot+}$ , of which the positive charge is localised on the phosphorus.

The absorption spectrum of **1a** measured in acetonitrile was different from that of triphenylmethane having a  $\pi$ -orbital as the HOMO, but similar to that of triphenylamine having an n-orbital as the HOMO. The difference of the absorption spectra among **1a**, triphenylmethane, and triphenylamine is the result of the different transition,<sup>7</sup>  $\pi$ - $\pi^*$  or n- $\pi^*$ .

### Laser flash photolysis

A time-resolved spectroscopic study using the laser flash photolysis technique was carried out to obtain information about the reaction intermediates. The transient absorption spectrum was observed in the laser flash photolysis (355 nm) of a mixture of **1** ( $1.0 \times 10^{-2} \text{ mol dm}^{-3}$ ) and DCA ( $5.0 \times 10^{-5} \text{ mol dm}^{-3}$ ) in argon-saturated acetonitrile containing  $0.10 \text{ mol dm}^{-3}$  of biphenyl (BP) as a co-sensitiser at room temperature. The oxidation potential 1.96 V of BP is higher than that of **1**, and the quantum yield ( $\phi_{\text{BP}^{\cdot+}} = 0.83$ ) of the BP radical cation ( $\text{BP}^{\cdot+}$ ) from the electron-transfer quenching of  $^1\text{DCA}^*$  by BP is particularly high.<sup>3</sup> Therefore, it is possible that  $\mathbf{1}^{\cdot+}$  is efficiently generated by hole transfer. In the absence of  $\text{BP}^{\cdot+}$ , the transient absorption spectrum of  $\mathbf{1}^{\cdot+}$  was not observed.

Three absorption bands around 350–400, 450–600, and 650–750 nm were observed at 100 ns after the flash, during laser flash photolysis of **1** in argon-saturated acetonitrile (Fig. 1). In oxygen-saturated acetonitrile, the absorption band around 650–750 nm disappeared. The absorption bands around 350–400 and 450–600 nm disappeared in the presence of  $5.0 \times 10^{-4} \text{ mol dm}^{-3}$  (*E*)-4,4'-dimethoxystilbene (DMS), while the absorption band 650–750 nm was not quenched. DMS was used as a radical cation scavenger to form a radical cation of DMS ( $\text{DMS}^{\cdot+}$ ), which showed a transient absorption at 530 nm. Therefore, the absorption band around 650–750 nm was assigned to  $\text{DCA}^{\cdot-}$ , and the absorption bands in the regions of 350–400 and 450–600 nm were assigned to  $\mathbf{1}^{\cdot+}$ . The absorption bands assigned to  $\mathbf{1}^{\cdot+}$  shifted to longer wavelengths with an increase in the electron-donating character of the *para* substituent.

Since DMS quantitatively quenched  $\mathbf{1}^{\cdot+}$  to give  $\text{DMS}^{\cdot+}$ , the quantum yield of the formation of  $\mathbf{1}^{\cdot+}$  was determined in the same manner as described in our previous paper.<sup>2b</sup> The quantum yield of the formation of  $\mathbf{1}^{\cdot+}$  decreased with an increase in the electron-donating character of the *para* substituent (Table 1).

### $\gamma$ -Radiolyses at 77 K

The assignments of radical cations can be confirmed by their absorption spectra observed during  $\gamma$ -radiolyses in *n*-butyl chloride rigid matrices at 77 K. It has been established that a substrate radical cation is effectively and selectively generated from the initial hole trapping process.<sup>8</sup> The absorption spectrum of  $\mathbf{1a}^{\cdot+}$  was observed with peaks at 375 and 510 nm during the  $\gamma$ -radiolysis of  $1.0 \times 10^{-2} \text{ mol dm}^{-3}$  **1a** in a *n*-butyl chloride rigid matrix at 77 K (Fig. 2a). On increasing the temperature (<90 K) without the formation of new absorption peaks, these peaks simply disappeared. The absorption spectra of  $\mathbf{1b-d}^{\cdot+}$  were also observed during  $\gamma$ -radiolysis under the same conditions already described (Fig. 2b–d). The absorption spectra of  $\mathbf{1a-d}^{\cdot+}$  observed during  $\gamma$ -radiolysis were similar to those observed during the laser flash photolysis of **1a–d** in oxygen-saturated acetonitrile, respectively.

## Discussion

### Photoinduced electron-transfer process

The DCA-sensitised photoinduced electron-transfer process of **1** is explained in Scheme 2. The electron transfer initially occurs

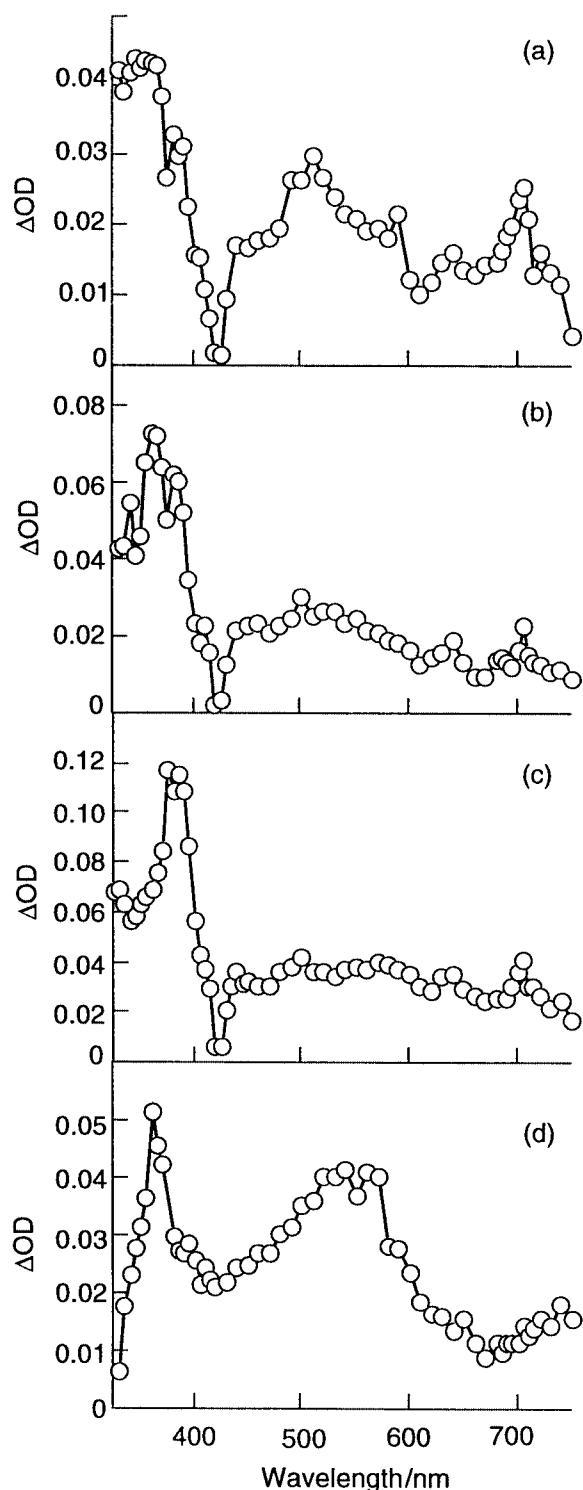


**Fig. 1** Transient absorption spectra observed at 100 ns after the laser pulse during 355 nm laser flash photolyses of the mixtures of  $1.0 \times 10^{-2} \text{ mol dm}^{-3}$  **1a-d** and  $5.0 \times 10^{-5} \text{ mol dm}^{-3}$  DCA in acetonitrile containing  $5.0 \times 10^{-2} \text{ mol dm}^{-3}$  biphenyl. (a)–(d) are spectra of **1a-d**, respectively.

from **1** to  $^1\text{DCA}^*$  to form the radical ion pair,  $[\mathbf{1}^{\cdot+}/\text{DCA}^{\cdot-}]$ , with  $1.8 \times 10^{10}$ – $2.3 \times 10^{10} \text{ dm}^3 \text{ mol}^{-1} \text{ s}^{-1}$  of the quenching rate constant  $k_q$ . The free energy changes  $\Delta G_{\text{et}}$  are in the region of  $-22.6$  to  $-30.9 \text{ kcal mol}^{-1}$ . These results indicate that the electron transfer from **1** to  $^1\text{DCA}^*$  occurs exergonically to give  $[\mathbf{1}^{\cdot+}/\text{DCA}^{\cdot-}]$  at the diffusion-controlled rate.

Formation of the radical ion was confirmed with the transient absorption measurement following the 355 nm laser flash photolysis. Electron transfer from **1** to  $^1\text{DCA}^*$  occurs to give  $\mathbf{1}^{\cdot+}$  and  $\text{DCA}^{\cdot-}$  during irradiation of the mixture of **1** and DCA in argon-saturated acetonitrile. The quantum yield of  $\mathbf{1}^{\cdot+}$

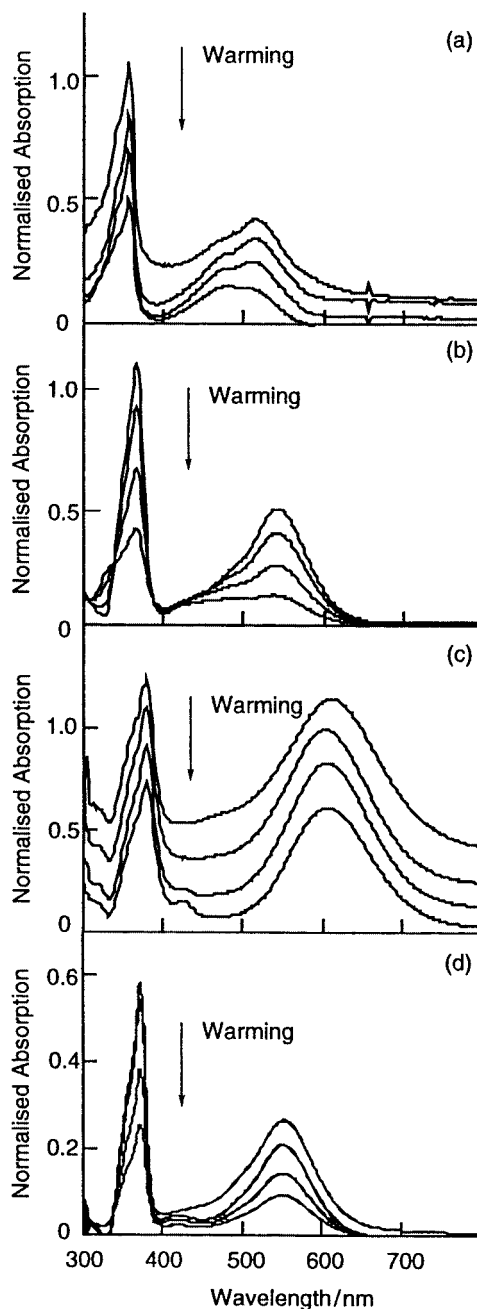
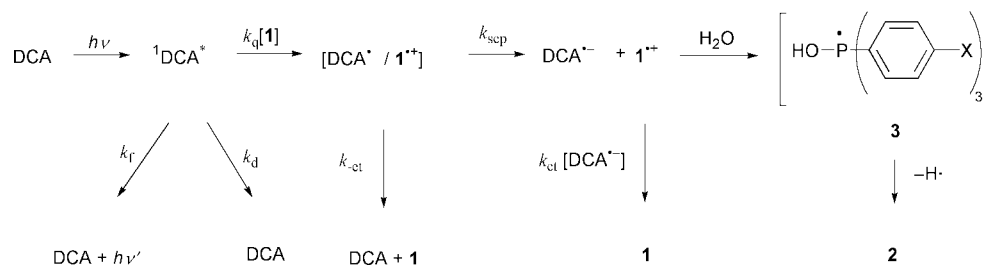


**Fig. 2** Absorption spectra observed after the  $\gamma$ -radiolysis of  $1.0 \times 10^{-2} \text{ mol dm}^{-3}$  **1a-d** in *n*-butyl chloride rigid matrices at 77 K and after warming. Arrows show decrease in the peak upon warming. (a)–(d) are spectra of **1a-d**, respectively.

decreased with an increase in the electron-donating character of the *para* substituent on the benzene ring (Table 1). The quantum yield of  $\mathbf{1}^{\cdot+}$  ( $\phi_{\mathbf{1}^{\cdot+}}$ ) described above is represented by  $\phi_{\mathbf{1}^{\cdot+}} = k_{\text{sep}}/(k_{\text{sep}} + k_{-\text{et}})$ , where  $k_{\text{sep}}$  is the rate constant for solvent separation and  $k_{-\text{et}}$  is the rate constant for back electron transfer. These two processes occur competitively in  $[\mathbf{1}^{\cdot+}/\text{DCA}^{\cdot-}]$  to give  $\mathbf{1}^{\cdot+}$  and  $\text{DCA}^{\cdot-}$  at  $k_{\text{sep}} = 5.0 \times 10^8 \text{ s}^{-1}$ , and **1** and DCA at  $k_{-\text{et}}$ .<sup>9</sup> The  $k_{-\text{et}}$  values of the present system were calculated from  $\phi_{\mathbf{1}^{\cdot+}}$  and  $k_{\text{sep}}$  (Table 1). Fig. 3 shows a plot of  $-\Delta G_{\text{et}}$  vs.  $\log k_{-\text{et}}$ . The plot indicates that the back electron transfer occurs in the inverted region.<sup>10</sup>

The oxidation potential of **1** shows that an electron is removed from the n-orbital of the phosphorus to give  $\mathbf{1}^{\cdot+}$ , of which the positive charge is localised on the phosphorus. The nucleophilic attack of  $\text{H}_2\text{O}$  towards the phosphorus of  $\mathbf{1}^{\cdot+}$  occurs to form phosphoranyl radical **3**.<sup>11</sup> Phosphine oxide **2** forms from  $\mathbf{1}^{\cdot+}$  with the quantum yields ( $\phi_2/\phi_{\mathbf{1}^{\cdot+}}$ ) of 0.52–0.15



Scheme 2

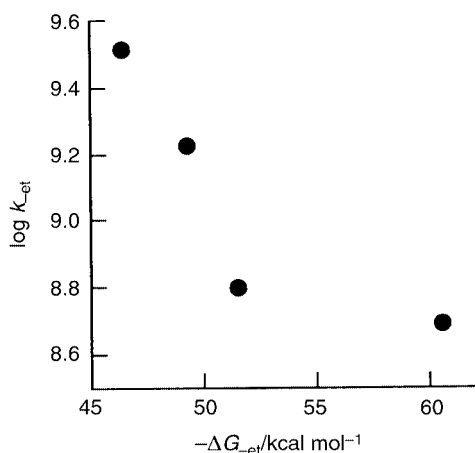


Fig. 3 Correlation between the free energy change ( $\Delta G_{-et}$ ) in the back electron transfer from  $\text{DCA}^{\cdot-}$  to  $\mathbf{1}^{\cdot+}$  and the rate of the back electron transfer ( $\log k_{-et}$ ).

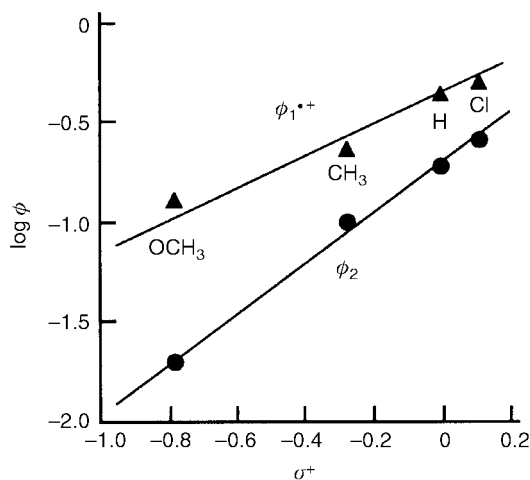


Fig. 4 Plots of the formation quantum yields of  $\mathbf{1}^{\cdot+}$  and  $\mathbf{2}$  versus the Brown-Okamoto  $\sigma^+$  parameter of the *para* substituents.

(Table 1). Since it is reasonable that the formation of  $\mathbf{2}$  from  $\mathbf{3}$  proceeds quantitatively,  $\phi_2/\phi_{1^{\cdot+}}$  is governed by the bimolecular reaction between  $\mathbf{1}^{\cdot+}$  and  $\text{H}_2\text{O}$ .

#### Substituent effect

The phosphine radical cation  $\mathbf{1}^{\cdot+}$  forms in  $\phi_{1^{\cdot+}} = 0.13\text{--}0.50$  and  $\mathbf{2}$  forms in  $\phi_2 = 0.02\text{--}0.26$ . Fig. 4 shows the plots of  $\log \phi_{1^{\cdot+}}$  and of  $\log \phi_2$  vs. the Brown-Okamoto  $\sigma^+$  parameters of the *para* substituents.<sup>12</sup> The linear correlations for  $\phi_{1^{\cdot+}}$  and  $\phi_2$  vs.  $\sigma^+$  gave the  $\rho$ -values of 0.67 (correlation coefficient  $r = 0.986$ ) and 1.25 ( $r = 0.997$ ), respectively. Therefore, the correlation between  $\log (\phi_2/\phi_{1^{\cdot+}})$  and  $\sigma^+$  was obtained with the  $\rho$ -value of 0.58 ( $r = 0.948$ ).

The substituent effect on the formation of  $\mathbf{1}^{\cdot+}$  depends on the back electron-transfer rate. Since the back electron transfer of  $[\mathbf{1c}^{\cdot+}/\text{DCA}^{\cdot-}]$  occurs at the rate constant of  $3.3 \times 10^9 \text{ s}^{-1}$  in the inverted region, the quantum yield of  $\mathbf{1c}^{\cdot+}$  having a

methoxy group on each benzene ring is the lowest. On the other hand, the quantum yield of  $\mathbf{2}$  is governed by the distribution of the positive charge in  $\mathbf{1}^{\cdot+}$ . Since the positive charge of the phosphorus atom of  $\mathbf{1c}^{\cdot+}$  is more delocalised than other  $\mathbf{1}^{\cdot+}$  radical cations, by conjugation with the  $\pi$ -electrons of the benzene ring and the n-electrons of the methoxy oxygen, the rate of the reaction of  $\mathbf{1c}^{\cdot+}$  with  $\text{H}_2\text{O}$  is smaller than that of the other  $\mathbf{1}^{\cdot+}$  radical cations. The delocalisation of the positive charge of  $\mathbf{1}^{\cdot+}$  may be related to the longer wavelength shift of the absorption bands of  $\mathbf{1}^{\cdot+}$  with an increase in the electron-donating character of the *para* substituent.

The positive  $\rho$  value calculated from the plot of  $\log (\phi_2/\phi_{1^{\cdot+}})$  vs.  $\sigma^+$  indicates that the formation of  $\mathbf{2}$  occurs through nucleophilic attack of  $\text{H}_2\text{O}$  on the positive charge of  $\mathbf{1}^{\cdot+}$ . Several substituent effects on photoinduced electron-transfer reactions have been reported.<sup>13</sup> For example, Dinnocenzo and co-workers have investigated the effect of *para* substituents in the reaction of the *para*-substituted phenylcyclopropane radical cation with methanol.<sup>13d</sup> From the Hammett plot, the  $\rho$  value can be estimated to be approximately 2.0, and is larger than the 0.58 in the present reaction of  $\mathbf{1}^{\cdot+}$  with  $\text{H}_2\text{O}$ . Since the HOMO of *para*-substituted phenylcyclopropane is the  $\pi$ -orbital of the phenyl group, the *para* substituent directly affects the oxidation of this  $\pi$ -orbital. The interaction of the C-C  $\sigma$ -bond of the cyclopropane ring with the  $\pi$ -orbital of the *para*-substituted phenyl group in the SOMO of the radical cation induces the reaction with methanol. In the present work, the *para* substituent of  $\mathbf{1}$  indirectly affects the oxidation of the n-orbital on the phosphorus atom through the benzene ring, which has an effect on the reaction of  $\mathbf{1}^{\cdot+}$  with  $\text{H}_2\text{O}$ . The extent of the positive charge delocalisation in  $\mathbf{1}^{\cdot+}$  by an electron-donating substituent is smaller than that in the *para*-substituted phenylcyclopropane radical cation, because it is indirect.

It has been reported that the Hammett equation gives a linear correlation between the substituents in the reactions of substituted triphenylphosphines with diazodiphenylmethane in acetonitrile.<sup>14</sup> The  $\rho$  value of the Hammett correlation has been calculated as  $-0.58$ . Since triphenylphosphine behaves as a nucleophile to diazodiphenylmethane, the  $\rho$  value is negative. The substituent has an influence on the nucleophilicity through the conjugation between the n-orbital of the phosphorus atom and the  $\pi$ -orbital of the phenyl group in the neutral triphenylphosphine. The absolute  $\rho$  value of this reaction is equal to that of the reaction of  $\mathbf{1}^{\cdot+}$  with  $\text{H}_2\text{O}$ .

#### Comparison with the photoinduced electron-transfer reaction of naphthyl phosphates

Recently we have reported that DCA sensitised the photoinduced electron-transfer reaction of tri-1-naphthyl phosphate, which is a pentavalent phosphorus compound.<sup>2</sup> One electron oxidation occurs on the naphthyl  $\pi$ -orbital, which is the HOMO, to form the radical cation of tri-1-naphthyl phosphate. This radical cation forms an intramolecular dimer radical cation from which the binaphthyl radical cation eliminates. No reaction occurs in the radical cations of 1,3-di-1-naphthylpropane and bis(1-naphthyl)oxy)methane, in which the two 1-naphthyl groups are linked by  $\text{CH}_2\text{--CH}_2\text{--CH}_2$  and  $\text{O--CH}_2\text{--O}$ , respectively. The O-P(O)-O spacer connecting two naphthyl

groups is responsible for the elimination of the binaphthyl radical cation. Since the HOMO of **1** is the n-orbital of the phosphorus atom, the n-electron of the phosphorus atom is oxidised to give  $\mathbf{1}^{+\cdot}$ . The *para* substituent on the benzene ring of  $\mathbf{1}^{+\cdot}$  affects the reactivity of  $\mathbf{1}^{+\cdot}$  with nucleophiles through the interaction of the  $\pi$ -orbital of the benzene ring with the n-orbital. This substituent effect is characteristic of triphenylphosphine radical cations.

## Conclusion

Nucleophilic attack of  $\text{H}_2\text{O}$  upon  $\mathbf{1}^{+\cdot}$  is the essential reaction in the formation of **2**. The quantum yields of  $\mathbf{1}^{+\cdot}$  ( $\phi_{\mathbf{1}^{+\cdot}} = 0.50\text{--}0.13$ ) and **2** ( $0.26\text{--}0.02$ ), which vary with the substituent on the benzene ring, are also determined in the present study. The quantum yield of  $\mathbf{1}^{+\cdot}$  depends on the rate of the back electron transfer in  $[\mathbf{1}^{+\cdot}/\text{DCA}^{\cdot-}]$ . The quantum yield of **2** is governed by the rate of the reaction of  $\mathbf{1}^{+\cdot}$  and  $\text{H}_2\text{O}$ ; in other words, by the density of the positive charge mainly localised on the phosphorus atom. The difference of the photoinduced electron-transfer reactions between *para*-substituted triphenylphosphine and tri-1-naphthyl phosphate is a consequence of the respective HOMO orbitals, which are the phosphorus non-bonding orbital and the naphthyl  $\pi$ -orbital, respectively.

## Experimental

### Apparatus

Melting points were obtained with a Yanagimoto micro point apparatus. UV-visible spectra were recorded on a Hitachi 150-20 spectrometer. Steady-state fluorescence spectra were recorded on a Hitachi 850 type fluorescence spectrometer.  $^1\text{H}$  and  $^{13}\text{C}$  NMR spectra were determined in  $\text{CDCl}_3$  with tetramethylsilane as an internal standard on a JEOL JNM-EX270 spectrometer. GLC analyses were carried out by use of a 2% Silicone OV-17 column. GC-MS spectra were recorded with a JMS-DX 300 instrument. HPLC analyses were carried out on a Shimadzu LC-10AS instrument with a Shiseido CAPCELL PAK C18 AG 120 column. Oxidation potentials were measured using a BAS CV-50W voltammetric analyser. Photoirradiation was carried out with a 300 W high-pressure mercury lamp, EHBW-300. Laser flash photolyses were carried out using the third-harmonic oscillation from a Nd:YAG laser (Quantel Model Brilliant). Low temperature  $\gamma$ -ray radiolyses were carried out using a  $^{60}\text{Co}$   $\gamma$  source (dose,  $2.6 \times 10^2$  Gy) at ISIR, Osaka University.

### Materials

The substrates **1a** and **2a**, purchased from Tokyo Chemical Industry Co., were used after recrystallisation from ethanol. The substrates **1b–d** were prepared from the corresponding phenylmagnesium bromide and phosphorus trichloride in dry tetrahydrofuran according to the method described in the previous paper.<sup>15</sup> Authentic samples of **2b–d** were also synthesised from the corresponding phenylmagnesium bromide and phosphorus oxychloride in tetrahydrofuran.

**Tris(4-methylphenyl)phosphine 1b.** Mp 146–147 °C (lit. 144–146 °C).<sup>15</sup>  $^1\text{H}$  NMR ( $\text{CDCl}_3$ ,  $\text{Me}_4\text{Si}$ )  $\delta = 7.22$  (2H, dd,  $J_{\text{HH}} = 6.0$  Hz,  $J_{\text{HP}} = 13.7$  Hz), 7.15 (2H, dd,  $J_{\text{HH}} = 6.0$  Hz,  $J_{\text{HP}} = 7.6$  Hz), and 2.34 (3H, s).  $^{13}\text{C}$  NMR ( $\text{CDCl}_3$ ,  $\text{Me}_4\text{Si}$ )  $\delta = 138.49$ , 134.14, 133.62, 129.24, and 21.30.

**Tris(4-methoxyphenyl)phosphine 1c.** Mp 133–134 °C (lit. 135 °C).<sup>15</sup>  $^1\text{H}$  NMR ( $\text{CDCl}_3$ ,  $\text{Me}_4\text{Si}$ )  $\delta = 7.23$  (2H, dd,  $J_{\text{HH}} = 7.5$  Hz,  $J_{\text{HP}} = 13.0$  Hz), 6.85 (2H, dd,  $J_{\text{HH}} = 7.5$  Hz,  $J_{\text{HP}} = 9.1$  Hz), and 3.79 (3H, s).  $^{13}\text{C}$  NMR ( $\text{CDCl}_3$ ,  $\text{Me}_4\text{Si}$ )  $\delta = 160.11$ , 134.94, 128.68, 114.15, and 55.17.

**Tris(4-chlorophenyl)phosphine 1d.** Mp 101–102 °C (lit. 102–105 °C).<sup>15</sup>  $^1\text{H}$  NMR ( $\text{CDCl}_3$ ,  $\text{Me}_4\text{Si}$ )  $\delta = 7.34$  (2H, dd,  $J_{\text{HH}} = 8.5$  Hz,  $J_{\text{HP}} = 7.5$  Hz) and 7.21 (2H, dd,  $J_{\text{HH}} = 8.5$  Hz,  $J_{\text{HP}} = 15.5$  Hz).  $^{13}\text{C}$  NMR ( $\text{CDCl}_3$ ,  $\text{Me}_4\text{Si}$ )  $\delta = 135.54$ , 134.81, 134.74, and 128.99.

**Tris(4-methylphenyl)phosphine oxide 2b.** Mp 146–147 °C (lit. 145 °C).<sup>16</sup>  $^1\text{H}$  NMR ( $\text{CDCl}_3$ ,  $\text{Me}_4\text{Si}$ )  $\delta = 7.54$  (2H, dd,  $J_{\text{HH}} = 8.1$  Hz,  $J_{\text{HP}} = 11.7$  Hz), 7.25 (2H, dd,  $J_{\text{HH}} = 8.1$  Hz,  $J_{\text{HP}} = 2.5$  Hz), and 2.39 (3H, s).  $^{13}\text{C}$  NMR ( $\text{CDCl}_3$ ,  $\text{Me}_4\text{Si}$ )  $\delta = 142.16$ , 132.00, 129.78, 128.90, and 21.51.

**Tris(4-methoxyphenyl)phosphine oxide 2c.** Mp 143–144 °C (lit. 143–144 °C).<sup>17</sup>  $^1\text{H}$  NMR ( $\text{CDCl}_3$ ,  $\text{Me}_4\text{Si}$ )  $\delta = 7.48$  (2H, dd,  $J_{\text{HH}} = 8.9$ ,  $J_{\text{HP}} = 11.9$  Hz), 6.95 (2H, dd,  $J_{\text{HH}} = 8.9$ ,  $J_{\text{HP}} = 2.3$  Hz), and 3.84 (3H, s).  $^{13}\text{C}$  NMR ( $\text{CDCl}_3$ ,  $\text{Me}_4\text{Si}$ )  $\delta = 165.11$ , 130.32, 127.71, 114.14, and 55.31.

**Tris(4-chlorophenyl)phosphine oxide 2d.** Mp 177–178 °C (lit. 177–178 °C).<sup>18</sup>  $^1\text{H}$  NMR ( $\text{CDCl}_3$ ,  $\text{Me}_4\text{Si}$ )  $\delta = 7.58$  (2H, dd,  $J_{\text{HH}} = 8.3$  Hz,  $J_{\text{HP}} = 11.6$  Hz) and 7.47 (2H, dd,  $J_{\text{HH}} = 8.3$  Hz,  $J_{\text{HP}} = 2.5$  Hz).  $^{13}\text{C}$  NMR ( $\text{CDCl}_3$ ,  $\text{Me}_4\text{Si}$ )  $\delta = 139.11$ , 133.28, 130.18, and 129.12.

### Photoirradiation procedure

A 3 cm<sup>3</sup> solution of a mixture of **1** ( $1.0 \times 10^{-2}$  mol dm<sup>-3</sup>) and DCA ( $5.0 \times 10^{-5}$  mol dm<sup>-3</sup>) was charged in a Pyrex tube (inner diameter 8 mm, 1 mm thick) and argon was bubbled through the solution to purge dissolved air. After irradiation with a high-pressure mercury lamp (300 W) under cooling with water (20–25 °C) using a  $\text{BiCl}_3/\text{HCl}$  solution filter (cutoff below 355 nm). The reaction mixture was analysed with HPLC and GLC and compared with authentic samples.

### Laser flash photolyses and $\gamma$ -ray radiolyses

Laser flash photolysis of the sample solutions was performed at room temperature by a flash at 355 nm (4 ns, 20 mJ pulse<sup>-1</sup>) obtained by the third-harmonic oscillation from a Nd:YAG laser. The probe beam was obtained from a 450 W Xe-lamp (Osram, XBO-450) synchronised with the laser flash. The probe beam was sent into the sample solution and focused to a computer-controlled monochromator (CVI Laser, Digikrom-240). The output of the monochromator was monitored by a PMT (photomultiplier tube; Hamamatsu Photonics, R1417 or R2497). The signal from the PMT was recorded on a transient digitiser (Tectronix, 7912AD with plug-ins, 7A19 and 7B92A). The signals were converted to transient optical densities.<sup>19</sup>  $\gamma$ -Radiolysis of **1** in degassed *n*-butyl chloride ( $10 \times 10^{-3}$  mol dm<sup>-3</sup>) at 77 K was performed in a 1.0 mm thick quartz cell using a  $^{60}\text{Co}$   $\gamma$  source for 30 min. Optical absorption spectra were taken by a spectrophotometer and a multichannel photodetector (Shimadzu, Multi Spec-1500).

### Acknowledgements

We thank the late Professor Setsuo Takamuku, Professor Yoshiki Okamoto, and the late Professor Reizo Dohno for their helpful discussion and Dr Akito Ishida, Ms Sachiko Tojo, Miss Tomoko Hashikawa, and Mr Masami Asai for their help in the experiments. This work was partly supported by a Grants-in-Aid for Scientific Research (Nos. 09226223, 10132237, 09450319, and 09875209) from the Ministry of Education, Science, Sport and Culture of Japan.

### References

- 1 R. L. Powell and C. D. Hall, *J. Am. Chem. Soc.*, 1969, **91**, 5403; G. Pandey, S. Hajra, M. K. Chorai and K. R. Kumar, *J. Am. Chem. Soc.*, 1997, **119**, 8777; G. Pandey, D. Pooranchand and U. T. Bhalariao, *Tetrahedron Lett.*, 1991, **47**, 1745; S. Yasui, K. Shioji, A. Ohno and M. Yoshihara, *J. Org. Chem.*, 1995, **60**, 2099.

- 2 (a) M. Nakamura, R. Dohno and T. Majima, *Chem. Commun.*, 1997, 1291; (b) M. Nakamura, R. Dohno and T. Majima, *J. Org. Chem.*, 1998, **63**, 6258.
- 3 I. R. Gould, D. Ege, J. E. Moser and S. Farid, *J. Am. Chem. Soc.*, 1990, **112**, 4290.
- 4 M. E. R. Marcondes, V. G. Toscano and R. G. Weiss, *J. Am. Chem. Soc.*, 1975, **97**, 4485.
- 5 D. Rehm and A. Weller, *Isr. J. Chem.*, 1970, **8**, 259; A. Weller, *Z. Phys. Chem. (Munich)*, 1982, **133**, 93.
- 6 M. Culcasi, Y. Berchadsky, G. Gronchi and P. Tordo, *J. Org. Chem.*, 1991, **56**, 3537.
- 7 J. Eriksen and C. S. Foote, *J. Phys. Chem.*, 1978, **82**, 2659; H. Goetz, F. Nerdel and K. H. Wiechel, *Justus Liebigs Ann. Chem.*, 1963, **665**, 1; W. R. Orndorff, R. C. Gibbs, S. A. McNulty and C. V. Shapiro, *J. Am. Chem. Soc.*, 1927, **49**, 1541; L. C. Anderson, *J. Am. Chem. Soc.*, 1928, **50**, 208; L. C. Anderson, *J. Am. Chem. Soc.*, 1929, **51**, 1889.
- 8 T. Shida and W. Hamill, *J. Chem. Phys.*, 1966, **44**, 2375; T. Shida, in *Electronic Absorption Spectra of Radical Ions*, Elsevier, Amsterdam, The Netherlands, 1988, p. 113; E. R. Klinshpont, in *Organic Radiation Chemistry Handbook*, ed. V. K. Milinchuk and V. I. Tupikov, Ellis Horwood, New York, 1989, p. 26; W. Hamill, in *Radical Ions*, ed. E. T. Kaiser and L. Kevan, New York Interscience, New York, 1968, p. 321.
- 9 A. Weller, *Z. Phys. Chem. (Munich)*, 1982, **130**, 129.
- 10 R. A. Marcus, *J. Chem. Phys.*, 1956, **24**, 966; R. A. Marcus, *Annu. Rev. Phys. Chem.*, 1964, **15**, 155.
- 11 W. G. Bentrude, in *Reactive Intermediates*, ed. R. A. Abramovitch, Plenum Press, New York, 1983, vol. 3, p. 199 and references cited therein.
- 12 H. C. Brown and Y. Okamoto, *J. Am. Chem. Soc.*, 1958, **80**, 4979.
- 13 For example: (a) K. Gollnick, A. Schnatterer and G. Utschick, *J. Org. Chem.*, 1993, **58**, 6049; (b) T. Karatsu, H. Itoh, T. Kinunaga, Y. Ebashi, H. Hotta and A. Kitamura, *J. Org. Chem.*, 1995, **60**, 8270; (c) J. P. Dinnocenzo, D. R. Lieberman and T. R. Simpson, *J. Am. Chem. Soc.*, 1993, **115**, 366; (d) J. P. Dinnocenzo, H. Zuillhof, D. R. Lieberman, T. R. Simpson and M. W. McKechney, *J. Am. Chem. Soc.*, 1997, **119**, 994.
- 14 D. Bethell, R. Bourne and M. Kasran, *J. Chem. Soc., Perkin Trans. 2*, 1994, 2081.
- 15 F. G. Mann and E. J. Chaplin, *J. Chem. Soc.*, 1937, 527.
- 16 A. Michaelis, *Justus Liebigs Ann. Chem.*, 1901, **315**, 43.
- 17 A. Seneor, W. Valient and J. Wirth, *J. Org. Chem.*, 1960, **25**, 2001.
- 18 G. P. Schiemenz, *Chem. Ber.*, 1966, **99**, 504.
- 19 S. Tojo, K. Morishima, A. Ishida, T. Majima, S. Takamuku, *Bull. Chem. Soc. Jpn.*, 1995, **68**, 958.